

PROCEEDINGS ICEM15

15th International Conference on Experimental Mechanics
15th ICEM - FUNDASSEM - AI/AF-1
Porto, 22-27 July 2012

Editors

J.F. Silva Gomes & Mário A.P. Vaz
(University of Porto)

Edições INEGI
2012
(ISBN: 978-972-8826-26-0)

ENTER

15th International Conference on Experimental Mechanics Porto/Portugal, 22-27 July 2012

Editors Preface

Engineering practice in general and mechanical design in particular are basically exercises of creativity, triggered by specific needs. As the engineering community continues to cross the boundaries of known practices, design and manufacturing techniques into the frontiers of new materials and mechanical systems, energy sources and their effects upon the environment, the opportunities for failure will inevitably increase. If our knowledge of how to engineer systems, structures and components to minimize or prevent failure is to keep pace with modern demanding applications and the intolerance of a safety conscious society, we must develop and apply superior analytical and experimental tools to evaluate the potential for damage or failure of engineering structures and/or components and the associated energy harvesting systems.

Different tools are available to optimize any engineering solution, from which *Experimental Mechanics* has always played a most prominent role. It is related to such diverse disciplines as physical and mechanical sciences, engineering (mechanical, aeronautical, civil, automotive, nuclear, etc.), materials, electronics, medicine and biology, and uses experimental methodologies to test and evaluate the behaviour and performance of all kinds of materials, structures and mechanical systems. Quality control, safety, destructive and non-destructive testing of materials and components, analysis of prototypes and even fundamental research are some of the possible applications of *Experimental Mechanics*. During the last few decades the development of computer based techniques, as well as laser-optics methods, nanotechnologies and nanomaterials, among many other technological advances, added new dimensions and perspectives to *Experimental Mechanics and Testing*.

This CD-ROM contains the 566 papers accepted for presentation in the ICEM15-15th International Conference on Experimental Mechanics held in Porto/Portugal, 22-27 July 2012. The different papers are organized in three main parts: PART-A, with the files of the 11 Invited Plenary Papers, by distinguished academics and scientists in the field of *Experimental Mechanics*; PART-B, with 289 papers distributed by the 12 general tracks/main topics (from A to L); and PART-C, with the remaining 266 papers from the 20 Special Symposia in ICEM15.

The ICEM15 conference is part of a prestigious series of conferences that was initiated in 1959, in Delft (The Netherlands), and the last one took place in Poitiers (France) in July 2010. All these *Experimental Mechanics* meetings resulted from the belief that of those disciplines associated with advanced product design and manufacture, experimental mechanics techniques have been making continuous and significant advances during the years. Important and dramatic improvements in systems and components design can be made by the use of the latest advances in experimental mechanics techniques applied to energy systems, structures and materials. Their effect on the environment is significant and will help in avoiding global warming and harmful CO₂ emissions.

It is organized by the Faculty of Engineering of the University of Porto (FEUP) and the Portuguese Association for Experimental Mechanics (APAET), under the auspices of the European Society for Experimental Mechanics (EURASEM), and sponsored by a number of national and international organizations, whose support is gratefully acknowledged: SEM-American Society for Experimental Mechanics, BSSM-British Society for Strain Measurement, JSME-Japanese Society of Mechanical Engineering, IMEKO-International Measurement Confederation, AFM-Association Française de Mécanique, DYMAT-European Association for Dynamics of Materials, INEGI-Instituto de Engenharia Mecânica e Gestão Industrial, LABIOMEPLaboratório de Biomecânica do Porto, LNEC-Laboratório Nacional de Engenharia Civil, FCT-Fundação para a Ciência e a Tecnologia, FCG-Fundação Calouste Gulbenkian, FLAD-Fundação Luso-Americana para o Desenvolvimento, CCDRN-Comissão de Coordenação e Desenvolvimento Regional do Norte, ABEU-PCO, Professional Congress Organizer, and Teatro Nacional S. João/Secretaria de Estado da Cultura.

We are particularly indebted to all *Symposium Promoters* for the coordination of the different themes and to the authors for their papers and presentations. The different contributions during the conference offered opportunities for thorough discussions with the authors. We acknowledge all of the participants, who contributed with innovations, new research approaches, novel techniques and testing methodologies, and their invaluable critical comments.

We are also indebted to the eleven outstanding *Plenary Lecturers* who highlighted the conference themes with their contributions: Dr. Shaker A. Meguid (University of Toronto/Canada), Dr. Gustavo B. Guimarães (Manufacture Engineering, EMBRAER/Brazil), Dr. Yoshiharu Morimoto (Moire Institute Inc., and Wakayama University, Wakayama, Japan), Dr. Emmanuel Gdoutos (Democritus University of Thrace, Greece), Dr. Robert A.W. Mines (University of Liverpool, United Kingdom), Dr. Sergei T. Mileiko (Russian Academy of Sciences, Russia), Dr. Michael B. Prime ((Los Alamos National Laboratory, USA), Dr. Mário A.P. Vaz (University of Porto, Portugal), Dr. Josef Eberhardsteiner (Vienna University of Technology, Austria), Dr. José Ygnacio Pastor (Technical University of Madrid, Spain), and Dr. Alfredo C. Campos (LNEC, Portugal).

Finally, we wish to express our gratitude to the members of the International Scientific Committee for reviewing the papers and the Proceedings, and to the members of the Local Conference Organizing Committee: António T. Marques, Paulo T. de Castro, A.J.M. Ferreira, Carlos C. António, Jorge Seabra, J.D. Rodrigues, Clito F. Afonso, Álvaro Cunha, Elsa Caetano, and Rui C. Barros, and the National Organizing Committee: João Ferreira (IST, Lisbon), Jorge Gomes (LNEC, Lisbon), José M. Cirne (UC, Coimbra), Paulo G. Piloto (IPB, Bragança), Mário Santos (LNEG, Lisbon).

Porto, July 2012

J.F. Silva Gomes and Mário A.P. Vaz

PAPER REF: 2809

EXPERIMENTAL TESTS OF PARTIALLY ENCASED BEAMS AT ELEVATED AND ROOM TEMPERATURE

Paulo A.G. Piloto^{1(*)}, Ana B.R. Gavilán², Luís M.R. Mesquita³, Luísa Barreira⁴, Carlos Gonçalves⁵

^{1,3,4,5}IDMEC^(*), Polytechnic Institute of Bragança, Bragança, Portugal

²Department of Mechanics, University of Salamanca, Zamora, Spain

^(*)Email: ppiloto@ipb.pt

ABSTRACT

This work presents the experimental tests developed on partially encased beams (PEB) at elevated temperature and room temperature. PEB were built with IPE100 steel profile. Two beam lengths were tested (2.5 and 4 m) at room, 400 and 600 °C. Seven series were tested to compare the performance of PEB using two different stirrups shear conditions (welded -W and not welded to web - NW). The behaviour of IPE 100 PEB was also compared with IPE 100 bare steel beam at room temperature. Most of the beams attained the ultimate limit state by lateral torsional buckling (LTB), with exception for those tested at 600 °C which collapsed by the formation of a plastic hinge (PH). The performance of each PEB was characterized based on some load events. The load value for plastic behaviour (F_{Mpl}), the load value for displacement equal to $L/30$ ($F_{L/30}$) and the load value for the ultimate load (F_u). The bending strength of the PEB at room temperature is almost two times the bending resistance of bare steel beam. The reduction on bending resistance of PEB is not directly proportional to the increase of temperature. An increase of temperature from room to 400°C and to 600°C leads to a reduction of 37 % and 64% on $F_{L/30}$, respectively. The ultimate load of PEB increased 85% in comparison with bare steel at room temperature. A decrease in the ultimate load of 24% and 22% was verified when temperature increased from room to 400 °C and from 400 °C to 600 °C, respectively. The bending resistance of PEB without welded stirrups slightly decreased in comparison to PEB with welded stirrups.

Keywords: Partially encased beams, Composite steel and concrete, Bending resistance, Elevated temperature

1- INTRODUCTION

Partially Encased Beams (PEB) are often defined from a steel profile, usually I-Shape or H-shape cross section, using reinforced concrete between flanges. Concrete between flanges increases fire resistance, load bearing and stiffness, without enlarging the overall size of bare steel cross sections. These advantages outweigh the increasing self-weight of the partially encased solution.

PEC (partially encased columns) were already tested at room and elevated temperatures. Hunaiti et al. (Hunaiti et al, 1994), analysed the behaviour of 19 PEC without additional shear connectors, and tested those with shear connectors and batten plates for different loading conditions. All columns presented full composite action and similar strength, regardless of the type of additional steel. Stefan Winter and Jörg Lange, (Stefan et al, 2000), determined the ultimate load of 8 PEC at room temperature using high strength-steel. Authors developed some full scale tests under fire conditions and concluded for equal ultimate load for both materials. Brent and Robert (Brent et al, 2006), investigated the behaviour of PEC, comparing

the performance of High Strength Concrete (HSC) and Normal Strength Concrete (NSC), evaluating the ultimate load and deformed shape mode. Authors verified that PEC with HSC had more brittle failure mode than NSC, concluding that introducing steel fibres and reducing spaces between stirrups would improve ductility. A. Correia and João P. Rodrigues (A. Correia et al, 2011), studied the effect of load level and thermal elongation restraint on PEC under fire conditions. They concluded that the surrounding stiffness had a major influence on fire element behaviour for lower load levels. The increasing of the surrounding stiffness is responsible for reducing critical time. Critical time remains practically unchanged for higher load levels.

Partially Encased Beams (PEB) have been widely tested at room temperature but only a small number of testes have been developed under fire or elevated conditions. The most relevant tests were developed by Kindmann et al (Kindmann et al, 1993), showing the importance of the reinforced concrete between flanges to determine the ultimate bending moment. This research caused the revision of Eurocode 4 (pre-standard) for the design of partially encased composite beams, to include the effect of the encased material for load bearing resistance and deflection calculations. Lindner and Budassis in 2000 (Lindner et al, 2000) developed a new design proposal for lateral torsional buckling, taking into consideration the torsional stiffness of concrete. Maquoi et al (Maquoi et al, 2002), improved the knowledge on the elastic critical moment and on the lateral torsional buckling resistant moment. Makamura et al. (Makamura et al, 2003), tested 3 partially encased girders with longitudinal and transversal rebars welded (W) and not welded (NW) to flanges, concluding that bending strength of the PEB was almost two times higher than conventional bare steel girders and specimens with rebar not welded to flanges presented a decrease of 15 % for maximum load bearing when compared to the welded rebar (W) specimens. Akio Kodaira et al. (Kodaira et al, 2004), determined the fire resistance of 8 PEB, with and without concrete slabs, showing that reinforcement is effective during fire. More recently, Piloto et al (Piloto et al, 2011) developed 15 experiments to calculate the fire resistance of PEB (small test series).

2- PARTIALLY ENCASED BEAMS

Partially encased sections achieve higher fire resistance when compared to bare steel sections. The increase in fire resistance is due to the encased material, reducing the exposed steel surface area, introducing concrete which has a low thermal conductivity. Higher fire resistance can also be achieved by increasing the amount of reinforcement to compensate for the reduction of steel strength in case of fire.

PEB were prepared by filling the space between the flanges of a steel IPE100 profile, using reinforced concrete (RC). Two different shear configurations for stirrups were used, both represented in figure 1. According to EN1994-1-1, (CEN, 2004), this composite steel and concrete section is classified as class 1.

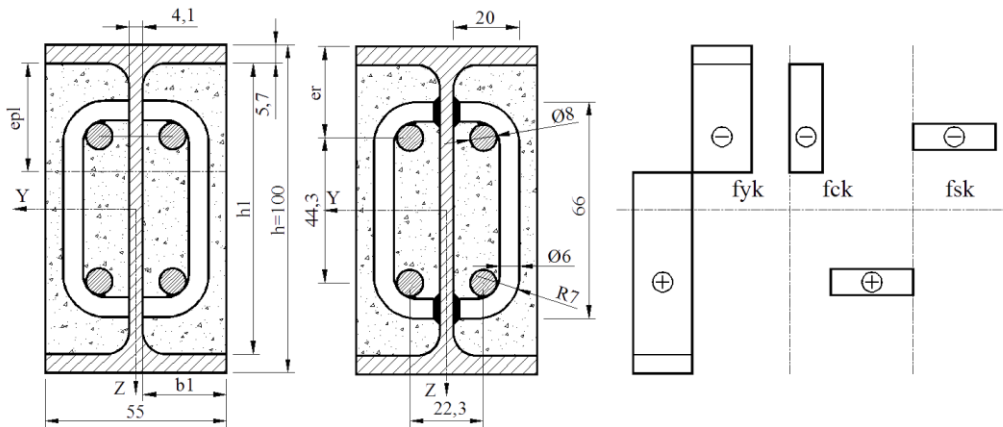


Fig.1 Cross section geometry and Plastic stress distribution.

The plastic neutral axis is referenced to “epI”, reinforced concrete block dimensions are represented by “b1” and “h1”, while “er” represents the relative position for reinforcement.

According to EN1994-1-2, (CEN, 2005), the analysis of structural elements under fire conditions may be carried out using either tabulated data, simplified or advanced calculation methods. Tabulated data refers only to composite beams rather than PEB, depends on load level, and is only valid for standard fire exposure and simple supporting conditions. A simple calculation method may be used to determine fire resistance of PEB without shear connection to the concrete slab. The rules for composite beams may be applied to PEB, assuming no mechanical resistance of the reinforced concrete slab, and establishing reduced effective areas of the cross section. An advanced calculation method may also be used to analyse partially encased beams. These models may include separate calculation programs for temperature and displacement.

In order to define load level dependence at room temperature, the plastic moment was calculated using characteristic values for material properties, assuming certain hypotheses based on stress field distribution, see figure 1 and eq. 1, (Lindner et al, 2000).

$$M_{pl} = W_{pl,y} \cdot f_{yk} - 2 \cdot f_{yk} \cdot t_w \cdot (0.5h_1 - e_{pl})^2 / 2 + f_{ck} \cdot 2 \cdot b_1 \cdot e_{pl} (0.5h_1 - 0.5e_{pl}) + 2 \cdot A_r \cdot (f_{sk} - f_{ck}) (h - 2 \cdot e_r) \quad (1)$$

The shear resistance was also verified at room temperature. The contribution of web encasement to shear may be taken into account if stirrups are fully welded to the web, otherwise shear reinforcement should not be considered. The contribution for the total shear resistance from steel resistance and RC resistance may be assumed to be in the same proportion as it is for bending resistance, (CEN, 2004). The design resistance for bending and shear were determined as 14.8 kNm and 102 kN, respectively. These values helped to decide about the capacity of the hydraulic jack to be used.

3- DESCRIPTION OF TESTS

Fourteen PEB and two bare steel beams were compared under four-point bending tests. Tests were grouped in seven series to determine bending resistance at different temperature levels. Two series were prepared to analyse the behaviour of shear condition of stirrups (not welded

to the web - NW), three series were prepared to analyse the behaviour at high temperature levels using welded stirrups (W) and two more series were defined to be tested at room temperature, comparing the composite solution with bare steel solution. Two slenderness ratios were considered, using beams with $L_t=2.5$ m and $L_t=4.0$ m, see table 1. This table identifies each PEB tested, the length between supports (L_s), the shear condition for stirrups, the maximum temperature used during heating and the maximum geometric imperfection. The initial out-of-straightness was measured using a laser beam.

Table 1 List of tested beams.

Series	Specimen	L_s [m]	Stirrups [W / NW]	Temperature [°C]	Maximum lat. Imper.[mm]
1	B/2.4-02	2.4	W	400	2
	B/2.4-03				2
2	B/2.4-07	2.4	NW	400	1
	B/2.4-09				1
3	B/3.9-01	3.9	W	400	2
	B/3.9-02				5
	B/3.9-03				3
4	B/3.9-04	3.9	W	600	2
	B/3.9-05				2
	B/3.9-06				5
5	B/3.9-07	3.9	NW	400	5
	B/3.9-09				2
6	B/3.9-11	3.9	W	room	2
	B/3.9-12				5
7	B/3.9-11A	3.9	-	room	1
	B/3.9-12A				3

Tests developed at room temperature used quasi-static load increments, based on load cell readings. Load was applied with two synchronized hydraulic jacks, see figure 2. Strain, displacement and cross section rotation were measured at central section (SM). Transversal and lateral displacements (ZG, YG) as well as cross section rotation were based on three wire potentiometric displacement transducers. Some important load events were recorded for each test. The load value for plastic moment (F_{Mpl}) was determined using the intersection method between two straight lines drawn from linear and non-linear interaction. The load event for transversal displacement equal to $L/30$ was also determined ($F_{L/30}$) and the maximum load level for the asymptotic behaviour of the transversal displacement was identified by (F_u).

Tests developed at elevated temperature used electro-ceramic heating device to increase and maintain temperature during loading. A heating rate of 800 °C/hour was applied, which led to heating periods of 15, 30 and 45 minutes. An insulation ceramic mat was applied to increase heating efficiency and to promote uniform temperature distribution. Free thermal elongation was allowed before adjusting both supports and starting with each test. Supports were adjusted and load was applied after temperature stabilization (60, 90 and 120 minutes, after the start of heating). The same procedure was used to measure transversal and lateral displacement, as well as cross section rotation. Load events were also recorded and temperature measurements stored for the main cross sections.

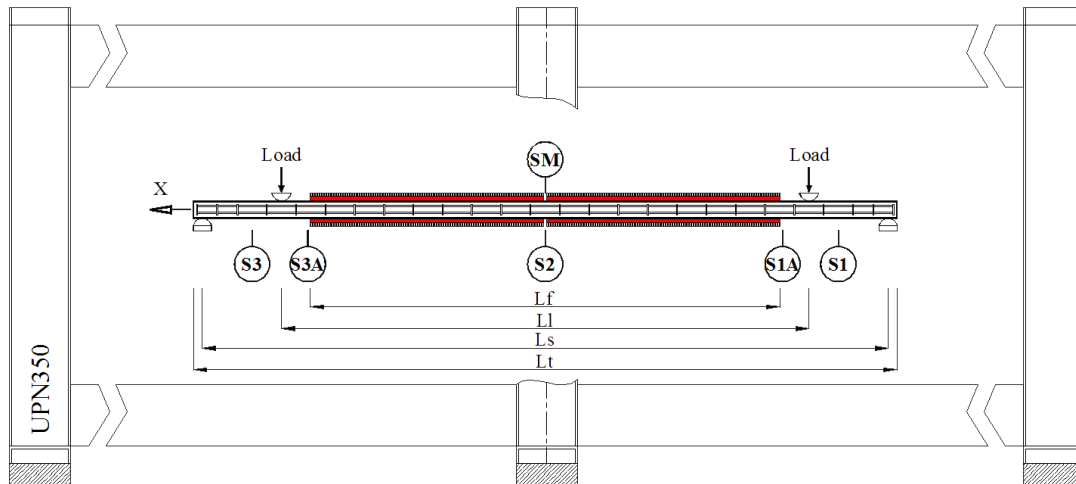


Fig.2 Testing conditions with main cross sections and reference lengths.

Five different cross sections were defined to measure temperature (S1, S1A, S2, S3A and S3), in case of elevated temperature tests and one cross section was used to measure strain (SM at room temperature), displacements (vertical Z_G , lateral Y_G) and cross section rotation θ_G .

Table 2 defines the main section and lengths used for testing medium and large series. The distance between load and support was kept constant for large and medium series. The length of specimens to be heated was shorter than the length between supports. This effect may be negligible because bending moment is reduced in the region nearest the supports and will not be affected by heating.

Table 2 Lengths defined for medium and large series (specimen).

Specimen	Total length Lt [m]	Length supports Ls [m]	Length load Ll [m]	Heating length Lf [m]
B/2.4	2.5	2.4	1.5	1.3
B/3.9	4.0	3.9	3.0	2.8

Two fork supports were applied on each four-point bending test. Restraint against Y/Z displacement and restraint against X rotation was considered at each support. A special interface was developed to apply vertical load, introducing a certain level of restraint against X rotation but allowing for lateral displacement Y. Teflon was used to reduce friction between the beam and the hydraulic jack and special grease applied at supports, see figure 3.



Fig.3 Load applied by the hydraulic jacks (left) and testing supports with load cell (right).

3.1- SPECIMEN PREPARATION

PEB were made of IPE100 using steel S275 JR, and C20 encased concrete with siliceous aggregates. Four longitudinal steel B500 rebar were used with diameter of 8 mm. Stirrups were designed with B500 rebar with a diameter of 6 mm, spaced every 167 mm. Stirrups were also partially welded to the longitudinal steel reinforcement, as represented in figure 4.



Fig.4 Specimens prepared for casting phase.

PEB were casted in the laboratory, without the need of formwork. Specimens were tested after more than 60 days, with respect to the first casting phase, to ensure normal bond adhesion. The second casting phase was performed one week after the first. This time delay did not influence the behaviour of PEB, because the second casting used the same concrete composition and the same environmental conditions. Both casting phases had sufficient cure time and concrete presented the same resistance in both stages.

The surface of materials had no special treatment and was used as delivered by manufacturers. Steel elements were cut from long steel bars, using traditional machinery. Stirrups were welded to the web of steel profile. Reinforcement was spot welded to stirrups in the case of

PEB with welded stirrups (W) and tied with wire rope in the case of PEB without welded stirrups (NW).

3.2- MATERIAL CHARACTERIZATION

Steel was characterized according to international standards (ISO, 2009) for hot rolled and cold formed steel, see table 3. Three samples were collected from the web of steel hot rolled profile and two more samples were collected from steel reinforcement.

Table 3 Tensile tests for hot rolled and cold formed steel.

Properties	Steel profile		Steel reinforcement	
	Average	Std. Deviation	Average	Std. Deviation
E [GPa]	197.901	2.948	203.294	2.110
R_{p,0.2%} [MPa]	300.738	6.720	524.993	3.521
ReH [MPa] (f_{yk}) (f_{sk})	302.466	5.749	531.508	7.908
ReL [MPa]	300.856	4.028	520.825	4.068
Rm [MPa] (fu)	431.252	5.020	626.574	11.539
At [%]	41.584	0.231	25.155	0.495

E- Elastic modulus, R_{p,0.2%}- proof strength for 0.2%, ReH- upper yield strength, ReL- lower yield strength, Rm- tensile strength, At- total extension at the moment of fracture.

Concrete was made with Portland cement, sand and siliceous aggregates. The concrete composition was prepared according to table 4. Aggregates (gravel and sand) were characterized by the sieving method and tested according to international standard (IPQ, 200) to determine particle size dimension. Due to the small size of the steel section and considering the offset dimension for the concrete cover of the stirrups, the concrete was made up with small-sized aggregates. The percentage of aggregates with diameters between 4-6 mm was approximately 90%, while the percentage of sand with diameters between 0.063-0.5 mm was 80%, see figure 5.

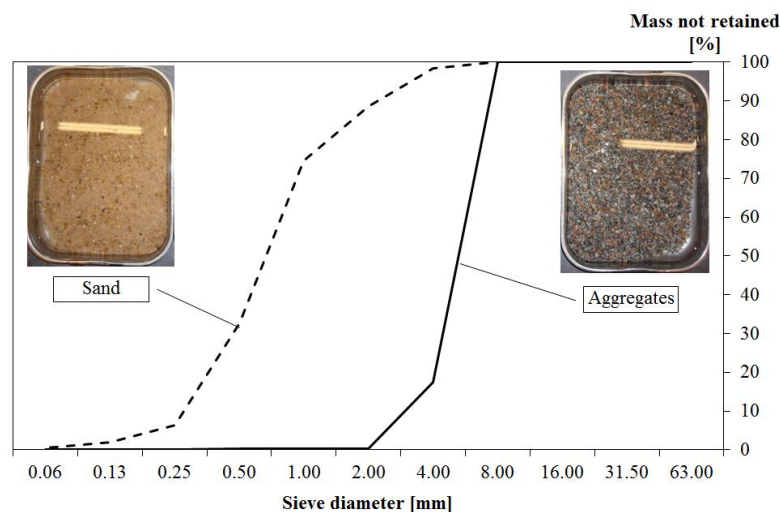


Fig.5 Results of sieving tests – Cumulative mass not retained.

The aggregate dimensions limit the value of the compressive resistance of concrete as concluded by Keru et al, (Keru et al, 2001). The high level of permeability at elevated

temperature was responsible for decreasing pore pressure. This fact justifies the absence of explosive spalling during experiments.

Table 4 Mix proportions of concrete.

Component for	1 [m ³] concrete
Sand	1322.7 [kg]
Aggregates	451.1 [kg]
Water	198 [l]
Cement	466.7 [kg]
Water / Cement	45 %

Table 5 shows the results for the compressive strength of concrete, using three compressive tests for cubic samples ($f_{ck,cube}$) and three compressive tests for cylindrical samples (f_{ck}).

Table 5 Mix proportions of concrete.

Properties	Cure [days]	Average	Std. Deviation
$f_{ck,cube}$ [MPa]	29	21.45	1.03
f_{ck} [MPa]	29	20.36	0.30

An increase of 100% on the compressive strength of concrete would lead to an increase of 2% in the bending resistance of PEB at room temperature (M_{pl}). This means that this section type is not sensitive to the value of the compressive strength of concrete.

3.3- INSTRUMENTATION

PEB were prepared to be tested at room temperature, measuring strain in central section (SM). Figure 6 represents the location for strain gauges, over steel flange and web, in hot rolled section (SM-WS and SM-OS) and over concrete (SM-RC1 and SM-RC2). Whereas perfect bond was considered between concrete and reinforcement, concrete strain was measured on steel reinforcement; for the latter measurement, rebars were machined 1 mm in depth and 15 mm in length, in respect to the dimensions of the electrical strain gauge. Five strain gauges (HBM reference 1-LY11-6/120) were used. All strain gauges were protected with gloss (Vishay reference M-coat A) and special viscous putty (HBM reference Ak22) against moisture, water and mechanical damage.

Strain gauges were also applied to bare steel beam, according to figure 7.

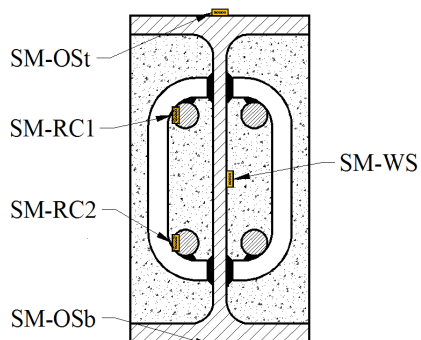


Fig.6 Strain gauge positions for PEB.

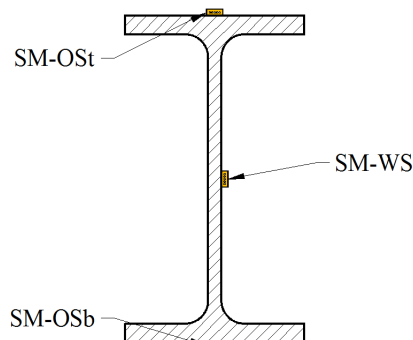


Fig.7 Strain gauge positions for bare steel beam.

Displacements were measured at the central section (SM) using three potentiometric wire displacement transducers.

For high temperature tests, thermocouples type K were positioned along the length of each element, according to figure 8. Thermocouples were spot welded to steel for measuring temperature in steel. Small steel washers were used to measure temperature of concrete, wrapping them in positions (Si-IC and Si-OC) during the casting phase.

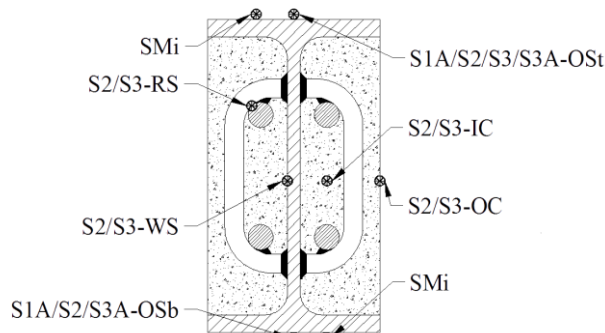


Fig.8 Thermocouple positions for all main sections.

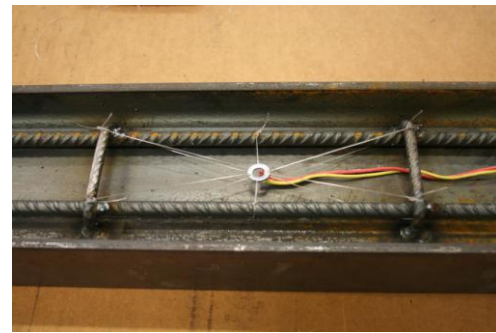


Fig.9 Thermocouple positions for position Si-IC.

Thermocouples were also used to control the electrical heating process. These thermocouples were directly connected to the control unit of the heating power centre (70 kW maximum power).

3.4- TEST PROGRAMME

Tests developed at room temperature used quasi-static load increments, based on load cell readings. Load was applied with two synchronized hydraulic jacks. Strain, displacement and cross section rotation were determined at central section (SM). Transversal and lateral displacements (Z_G , Y_G) as well as cross section rotation were based on three wire potentiometric displacement transducers. Some important force events were recorded during each test (F_{Mpl} , $F_{L/30}$, and F_u).

Figures 10 and 11 represent the deformed shape mode, at the end of tests B/3.9-11 and B/3.9-11A, respectively.

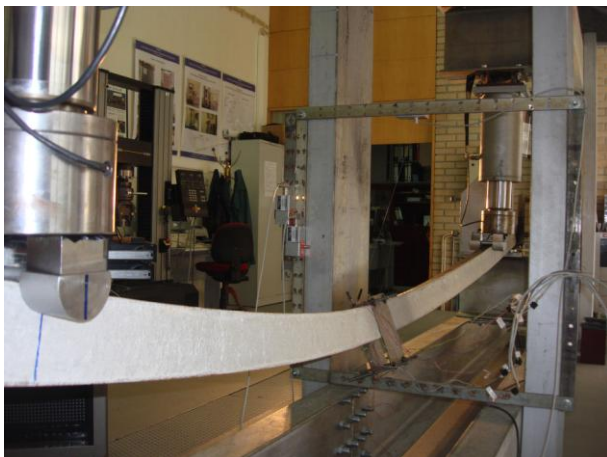


Fig.10 End of the test B/3.9-11.



Fig.11 End of the test B/3.9-11A.

Tests developed at elevated temperature used electro-ceramic heating device to increase and sustain temperature during loading. The heating device has a heat power unit with 70 (kVA) of maximum power. This device is able to deliver heat by the Joule effect, using special electro-ceramic resistances. The control unit reads, in real time, the temperature of two and four points (not represented), for medium and large test series, respectively. The same procedure was used to measure transversal and lateral displacement, as well as, cross section rotation. Load and temperature was recorded during each test.

Figures 12 and 13 represent the deformed shape mode, at the end of tests B/2.4-02 and B/3.9-06, respectively.



Fig.12 End of the test B/2.4-02.



Fig.13 End of the test B/3.9-06.

4- RESULTS

Next sessions present the results for medium and large series. The most important load events were recorded. Vertical displacement is compared with the large displacement criterion ($L/30$). Lateral displacement is also plotted for each beam test. Strain was recorded to acknowledge the elastic and plastic behaviour of the central section.

Time history temperature evolution demonstrates the stationary thermal load during the second stage of mechanical loading. Some typical thermography images also confirm the temperature distribution over the beam length.

4.1- RESULTS FOR MEDIUM SERIES

The main load events on medium series are represented on table 6. The load for plastic behaviour (F_{Mpl}) and the load for displacement criterion ($F_{L/30}$) are almost equal for every tested PEB. The maximum load (F_u) for series 1 is slightly higher in comparison with the same result for series 2.

Table 6 Load events for tests on medium series.

Series	Specimen	F_{Mpl} [N]	$F_{L/30}$ [N]	F_u [N]
1	B/2.4-02	21760	26583	31533
	B/2.4-03	19920	24878	33568
2	B/2.4-07	20610	24898	29000
	B/2.4-09	20850	25722	33246

Figure 14 represents the vertical displacement for both test series. Results agree very well with exception to the behaviour at higher and ultimate loads.

Figure 15 represents lateral displacement during each test. As expected, lateral displacement is almost null for most part of the test and finally starts to increase in simultaneous with cross section rotation.

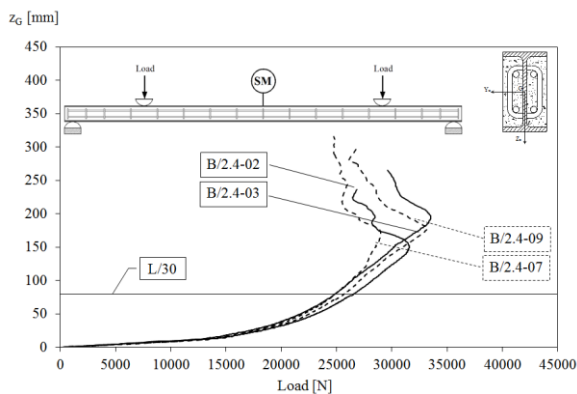


Fig.14 Deflection at mid span for series 1/2.

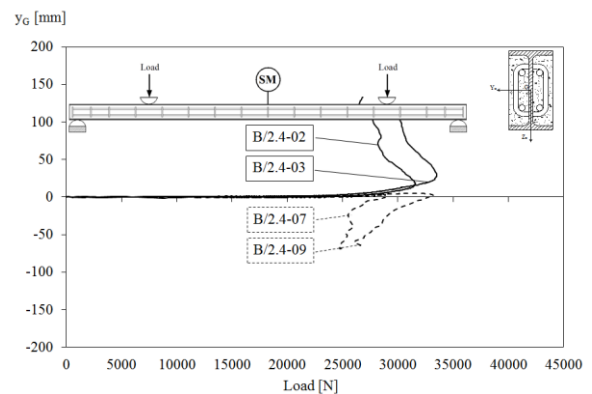


Fig.15 Lateral displacement for series 1/2.

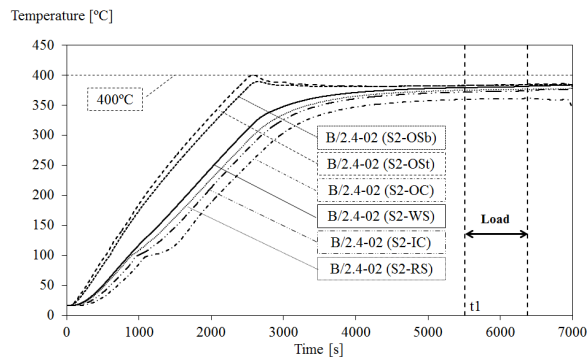


Fig.16 Heating for test B/2.4-02, section S2.

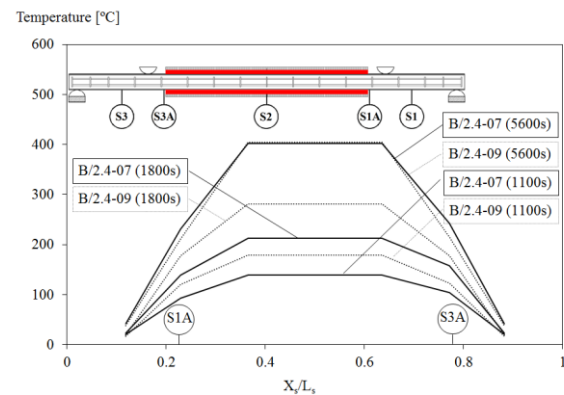


Fig.17 Temp. distribution and evolution for series 2.

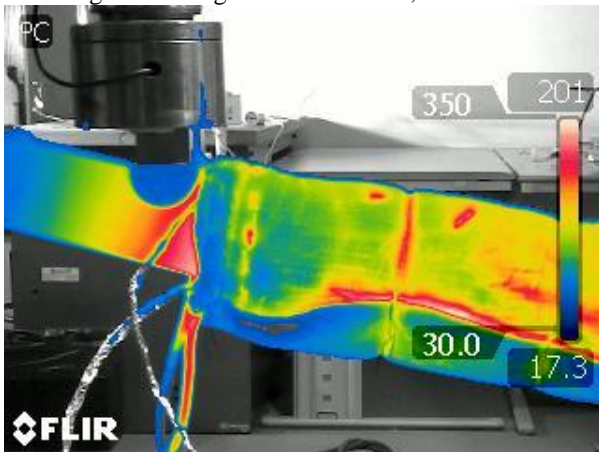


Fig.18 End of the test B/2.4-03.

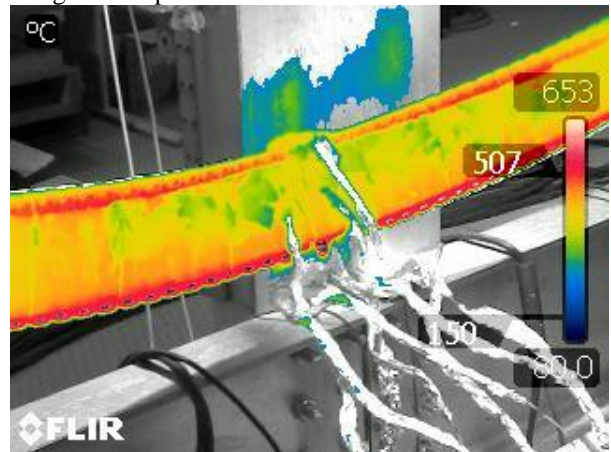


Fig.19 After the end of the test B/2.4-03.

The time history heating process is represented in figures 16 and 17. The moisture of concrete evaporates and produces some temperature inflection on concrete measurements. Temperature is not uniform along the length of the beams due to heat flow from central sections to extremities (supports) and also due to the reduced insulation near beam extremities.

Figures 18 represent the temperature measured in the external surface of the insulation and also between load and support.

At the end of the tests, the insulation material was removed and thermography proved an almost constant value of temperature along heating length (Lf).

4.2- RESULTS FOR LARGE SERIES

The main load events on large series are represented on table 7. Results agree very well for the first two main load events, with exception for the ultimate load (Fu). Differences may be explained by the friction effect near the support and load and by the deformation mode shape developed at high load level.

Table 7 Load events for tests on medium series.

Series	Specimen	F _{Mpl} [N]	F _{L/30} [N]	F _u [N]
4	B/3.9-01	16370	22126	30204
	B/3.9-02	16360	22715	27290
	B/3.9-03	14850	22573	28337
5	B/3.9-04	9620	12641	22456
	B/3.9-05	9759	12996	21662
	B/3.9-06	9110	12025	22770
6	B/3.9-07	15000	22665	23591
	B/3.9-09	15100	23207	24816
7	B/3.9-11	31600	35428	38718
	B/3.9-12	32100	36161	36380
8	B/3.9-11A	-	-	19436
	B/3.9-12A	-	-	21272

Figures 20-21 present the results for transversal and lateral displacements. Results agree very well with each other, with exception to the end of the tests. Bending resistance decreases with temperature.

Similar results were determined for the time history of every high temperature series. The moisture effect on concrete temperature is also represented. Temperature is not uniform along the length of the beams due the same reasons explained before.

Figures 24 and 25 present the thermography results during the test and after the end of the test, as well. Spatial gradient is visible along the extremity of the beam.

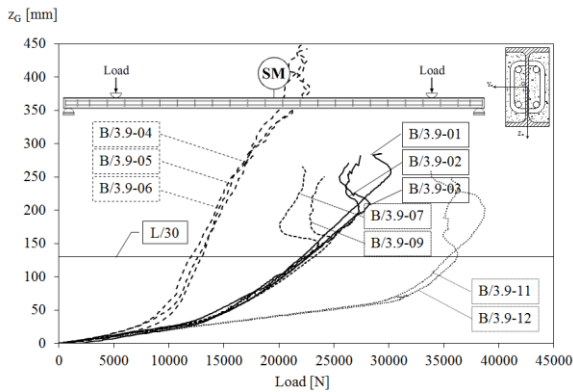


Fig.20 Deflection at mid span for series 3/4/5/6.

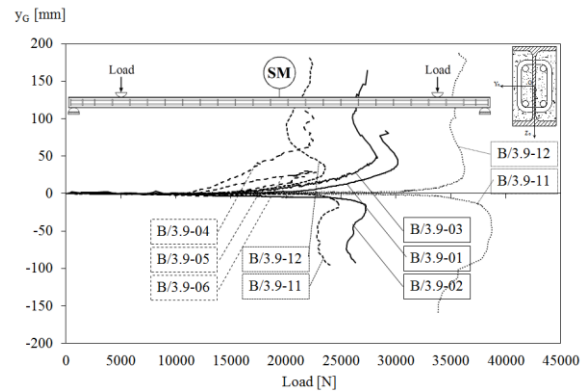


Fig.21 Lateral displacement for series 3/4/5/6.

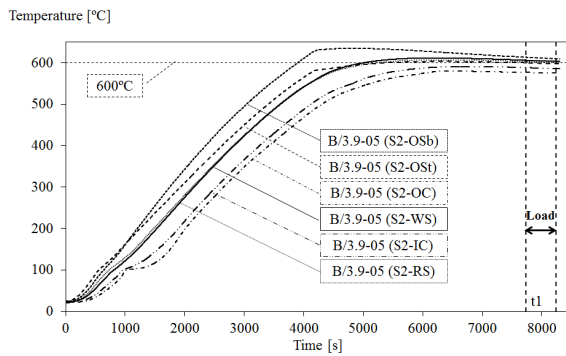


Fig.22 Heating for test B/3.9-05, section S2.

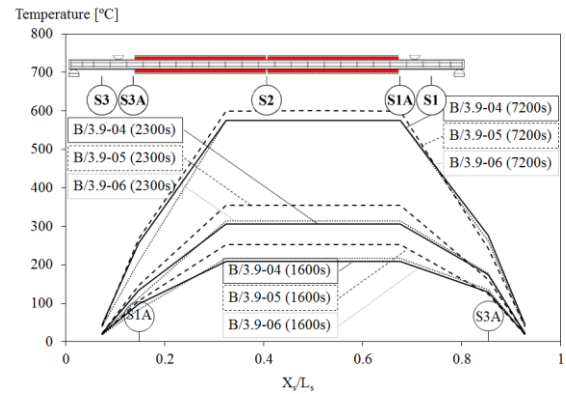


Fig.23 Temp. distribution and evolution for series 4.

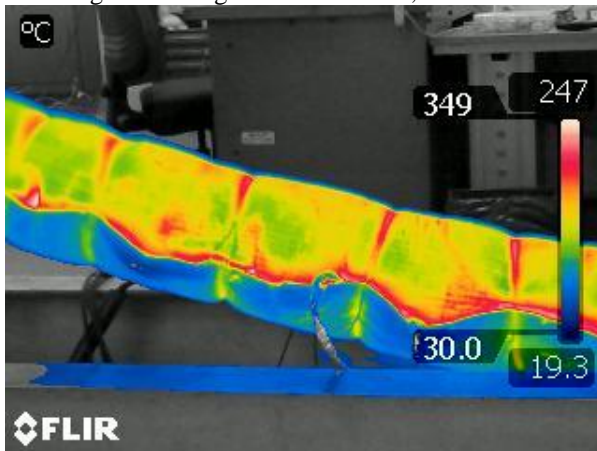


Fig.24 End of the test B/3.9-05.

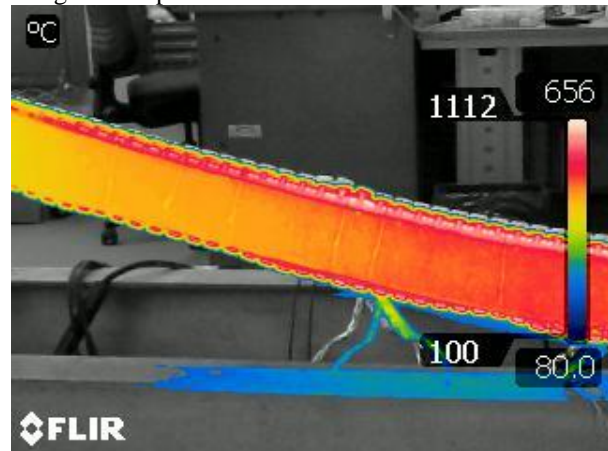


Fig.25 After the end of the test B/3.9-05.

PEB were also compared with bare steel beam, using the same steel profile. The deflection behaviour is very different besides both attained the lateral torsional buckling as deformed shape mode, see figure 26. The bending stiffness is also higher for the case of PEB.

Bare steel beams behaved on the elastic domain, as verified by the strain records, see figures 28 and 29. The steel elastic limit of the profile is also plotted on both graphs.

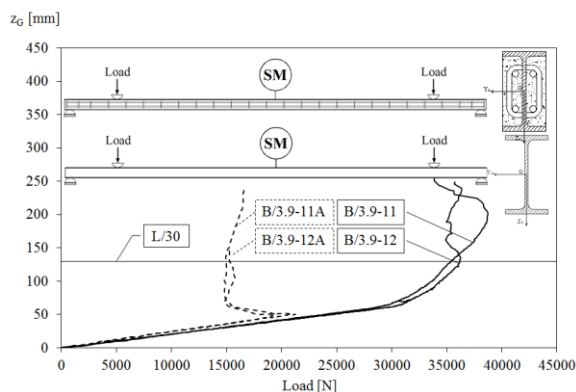


Fig.26 Deflection at mid span for series 6/7.

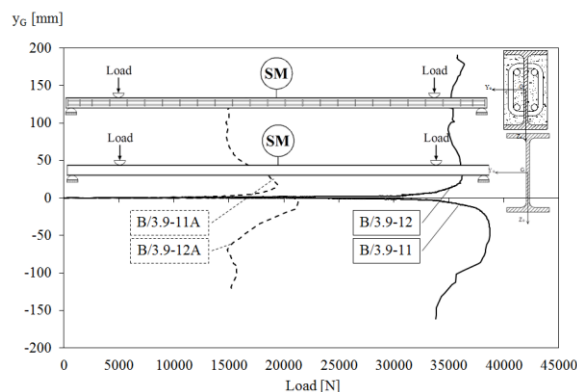


Fig.27 Lateral displacement for series 6/7.

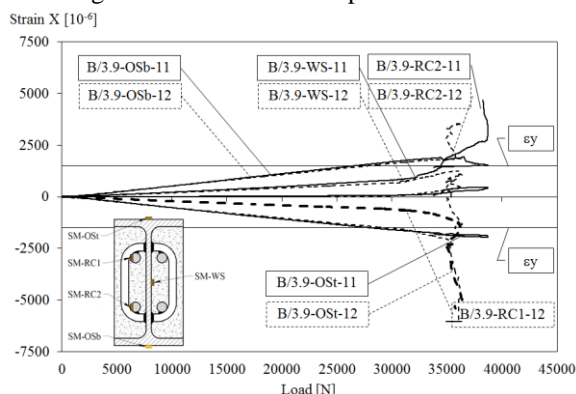


Fig.28 Strain X for series 6, section SM.

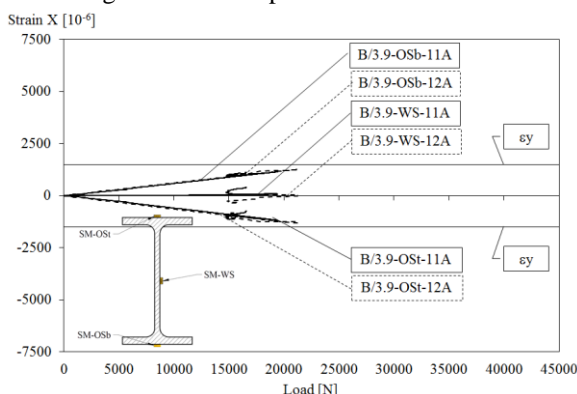


Fig.29 Strain X for series 7, section SM.

CONCLUSION

Four-point bending tests were performed to evaluate bending resistance of PEB at high and room temperature. Load and displacement results are presented to compare bending resistance. The bending resistance of the PEB at room temperature is almost two times the bending resistance of bare steel beam. The reduction on bending resistance of PEB is not directly proportional to the increase of temperature. An increase of temperature from room to 400°C and 600°C leads to a reduction of 37 % and 64% on $F_{L/30}$ criterion, respectively.

The deformed shape mode was LTB for all tested PEB and bare steel beams, with exception to those tested at 600 °C. For the last case the formation of a plastic hinge seemed to be the deformed shape mode, including a small amount of lateral displacement.

The deformation of large bare steel beams is completely different from PEB. The former series attained the ultimate limit state in the elastic range of material.

The bending stiffness of PEB is 15% higher than the bending stiffness of bare steel beam, at room temperature.

ACKNOWLEDGMENTS

The authors gratefully acknowledge the material support of the following companies: Arcelor – Mittal (Spain), J. Soares Correia (Portugal), Fepronor (Portugal) and Hierros Furquet (Spain).

REFERENCES

- Akio Kodaira, Hideo Fujinaka, Hirokazu Ohashi and Toshihiko Nishimura; "Fire Resistance of Composite Beams Composed of Rolled Steel Profile Concreted Between Flanges"; *Fire Science and Technology* Vol.23 No.3, pp. 192-208, 2004.
- Brent Prickett, Robert Driver, "Behaviour of partially encased composite columns made with high performance concrete", *Structural Engineering report n° 262*, University of Alberta, Department of Civil & Environmental Engineering, 2006.
- CEN - EN 1994-1-1; "Eurocode 4: Design of composite steel and concrete structures - Part 1-1: General rules and rules for buildings"; Brussels, December 2004.
- CEN - EN 1994-1-2; "Eurocode 4: Design of composite steel and concrete structures - Part 1-2: General rules - Structural fire design"; Brussels, August 2005
- Hunaiti, Y.; Fattah, B. A.; "Design considerations of partially encased composite columns", *Proceedings Institution of Civil Engineers Structures & Buildings*, v.106, pp.75-82, Feb. 1994.
- IPQ (Instituto Português da Qualidade), NP EN 933-1, "Tests for geometrical properties of aggregates – part 1; Determination of particle size distribution, sieving method", 2000.
- ISO TC 164, ISO 6892-1; "Metallic materials – tensile testing – part 1: Method of test at room temperature"; Switzerland, international standard, 2009.
- Joachim Lindner, Nikos Budassis; "Lateral torsional buckling of partially encased composite beams without concrete slab"; *Composite construction in steel and concrete IV*, conference proceedings, May 28th to June 2nd, Banff, Alberta, Canada, 2000.
- Keru Wu, Bing Chen, Wu Yao, Study of the influence of aggregate size distribution on mechanical properties of concrete by acoustic emission technique, *Cement and Concrete Research*, Volume 31, Issue 6, pp. 919-923, May 2001.
- Paulo A. G. Piloto, Ana B. R. Gavilán, Luís M. R. Mesquita; "Temperature analysis on fire resistance experiments of partially encased beams"; *Safety and Security Engineering IV*, pp. 313- 324, WIT Press, ISBN 978-1-84564-522-9, ISSN: 1746-4498 (PRINT), ISSN:1743-3509 (ON-LINE), University of Antwerp, Belgium, 4-6 July 2011.
- R. Kindmann, R. Bergmann, L—G. Cajot, J. B. Scleich; "Effect of reinforced concrete between the flanges of the steel profile of partially encased composite beam"; *Journal of Constructional Steel Research*, 27, pp 107-122, 1993.
- R. Maquoi, C. Heck, V. Ville de Goyet, et al, (European commission), "Lateral torsional buckling in steel and composite beams"; ISBN 92-894-6414-3; Book 1,2 and 3; *Technical steel research final report EUR 20888 EN*; August 2002.
- S. Nakamura, N. Narita, "Bending and shear strengths of partially encased composite I-girders", *Journal of Constructional Steel Research*, 59, pp.1435-1453, 2003.
- Stefan Winter and Jörg Lange, "Behavior of Partially Encased Composite Columns Using High-Strength Steel – Service and Fire Condition", *Proceedings of the Conference, "Composite Construction IV"*, Banff, Canada, 2000.